Research on State of Charge (SOC) Estimation of Gel Lithium Battery Based on Multi-Dimensional Ultrasonic Time-Frequency Characteristics

Haiyan Qiao , Guoliang Zhao * , Mengmeng Liu , Hua Wang , Suzhen Liu

Posted Date: 21 April 2026

doi: 10.20944/preprints202604.1476.v1

Keywords: gel battery; state of charge; estimation; ultrasonic test

 doi:10.20944/preprints202604.1476.v1

Article

Research on State of Charge (SOC) Estimation of Gel Lithium Battery Based on Multi-Dimensional Ultrasonic Time-Frequency Characteristics

Haiyan Qiao [1], Guoliang Zhao [1,*], Mengmeng Liu [1], Hua Wang [1] and Suzhen Liu [2]

[1] School of Information and Electrical Engineering, Hebei University of Engineering, Handan City, Hebei Province, China

[2] School of Electrical Engineering, Hebei University of Technology, Tianjin City, China

* Correspondence: zhaoguoliang@hebeu.edu.cn

Abstract

Gel electrolyte batteries have prominent advantages in safety, service life and environmental adaptability, leading to their increasing application in various fields. Compared with liquid electrolyte batteries, gel batteries exhibit excellent internal resistance consistency, which contributes to more stable current, gentler voltage changes and lower temperature rise during charging and discharging processes. However, traditional methods for estimating the SOC of gel batteries based on electrical and temperature parameters fail to achieve satisfactory accuracy due to the aforementioned characteristics. To address this issue, this paper considers the changes in the physical properties of the electrolyte during the charging and discharging of gel batteries, investigates their multi-layer structure and analyzes the feasibility of SOC estimation using ultrasonic technology. Through ultrasonic experiments, the characteristic parameters in ultrasonic time-frequency signals that are highly correlated with the SOC of gel batteries are extracted and analyzed. Subsequently, based on machine learning algorithms, a SOC estimation method for gel batteries using multi-dimensional ultrasonic time-frequency features is proposed. The verification experiments show that the RMSE and MAE of this estimation results are both within 1% which confirm the effectiveness and high accuracy of the proposed method.

Keywords: gel battery; state of charge; estimation; ultrasonic test

1. Introduction

SOC is defined as the percentage ratio of the remaining dischargeable capacity of a battery to its total available capacity at the fully charged state [1]. For instance, a battery with a full-charge capacity of 80 kWh and a residual capacity of 40 kWh corresponds to an SOC of 50%. The charging and discharging operations of lithium battery must be strictly controlled within the allowable SOC range, since both overcharging and overdischarging can cause irreversible degradation to the battery. Typical degradation mechanisms include accelerated decomposition of the electrolyte, persistent structural collapse of electrode materials, and even thermal runaway [2–4]. Therefore, accurate SOC estimation is directly related to the operational safety and reliability of lithium battery systems [5].

Current mainstream SOC estimation methods include the coulomb counting method, open-circuit voltage (OCV) method, impedance-based method, model-based filtering algorithms and data-driven method [6,7]. Among emerging non-invasive techniques, the ultrasonic method has attracted extensive attention owing to its non-electrochemical interference, high sensitivity to the internal states of battery and considerable potential for online monitoring [8].

Existing studies have demonstrated that the intercalation and deintercalation of lithium ions between the cathode and anode during the charging and discharging process of lithium battery induce variations in the physical properties of the internal materials of the battery. Among these

 doi:10.20944/preprints202604.1476.v1

variations, the most prominent are the changes in the Young's modulus and density of the cathode and anode materials. Accordingly, the evolution of the internal state of a lithium battery is closely correlated with the structural characteristics of its constituent materials [9]. Exploring the variation law of the internal material structure of the battery during charging and discharging cycles and further applying this law to achieve accurate SOC estimation constitutes the research idea for ultrasonic monitoring. As a type of stress wave, ultrasonic waves propagating inside a battery are sensitive to subtle physical variations in the propagation medium, which further lead to changes in key propagation parameters such as wave velocity. Based on this acoustic-mechanical coupling mechanism, the response characteristics of ultrasonic waves can be employed to achieve real-time, in-situ and non-destructive characterization of the internal states of lithium battery. To date, researchers in this field have mainly adopted two time-domain characteristic parameters of ultrasonic signals - Time of Flight (*TOF*) and Signal Amplitude (*SA*) - for the quantitative estimation of the SOC [10,11].

By analyzing the variations in the density and Young's modulus of the cathode and anode materials of lithium battery, Hsieh A G et al. establish the correlation between ultrasonic wave velocity and battery SOC and they verify the existence of a linear relationship between *TOF* and SOC [12]. Then, based on the Biot fluid-saturated porous medium model, the ultrasonic propagation characteristics inside lithium battery are systematically investigated and an approximately linear correlation model between *SA* and SOC is constructed [13]. Studies further reveal that *TOF* and *SA* exhibit a strong correlation with the charge-discharge cycling process and aging degree of lithium battery [14]. By establishing an ultrasonic analytical model and simulating the dynamic variations in Young's modulus and density of battery electrodes during cycling, the reliability of this strong correlation is verified repetitively. Furthermore, several researchers have carried out comprehensive studies by combining *TOF*, *SA* and electrical parameters (e.g., battery voltage), and thus constructed a multi-dimensional ultrasonic - electrical fusion model for SOC estimation. The estimation error of this type of model can be constrained within 2% [15]. Moreover, the integration of tracking algorithms into this multi-dimensional model enables a further improvement in the accuracy of SOC estimation [16]. It should be noted that the aforementioned research achievements are almost exclusively obtained based on liquid electrolyte lithium battery. In contrast, research focusing on gel electrolyte lithium battery remains relatively scarce.

Gel electrolyte lithium battery represents an improved variant of traditional lithium battery. By confining liquid electrolytes within a polymer gel network, a semi-solid gel electrolyte is formed, which can effectively mitigate the leakage issue of liquid electrolytes, suppress thermal runaway-induced failures and enhance cycling stability. Gel electrolyte enhances the operational performance of lithium battery, making its ultrasonic linear characteristics extremely stable during charging and discharging. However, compared with traditional lithium battery, gel battery's internal structure and electrochemical behaviors are more complex, leading to nonlinear characteristics. When ultrasonic waves propagate inside gel electrolyte lithium battery, the nonlinear and non-stationary characteristics of the propagation process become particularly prominent. Thus, unlike the case of liquid electrolyte lithium battery, relying solely on time-domain analysis parameters such as *TOF* and *SA* is insufficient to accurately characterize the internal state of gel electrolyte lithium battery.

To achieve accurate SOC estimation for gel lithium battery, this study builds on existing research and collects ultrasonic signals during the battery's charge-discharge process. These signals are firstly analyzed in the time domain to extract *TOF* and *SA*. Subsequently, the frequency spectrum of the signals is obtained through Fourier transform. Further, Ensemble Empirical Mode Decomposition (EEMD) is employed to extract characteristic parameters, including slope, kurtosis, shape index, and pulse index - from the Intrinsic Mode Functions (IMFs) of the signals. Based on these multi-dimensional parameters, an attempt is made to interpret the internal electrochemical processes of the battery. Finally, a neural network algorithm is adopted for feature selection of the extracted parameters, and a precise SOC estimation method for gel lithium battery is proposed.

 doi:10.20944/preprints202604.1476.v1

2. Results and Discussion

2.1. Theoretical Analysis on Ultrasonic Characterization of SOC

The propagation velocity of an ultrasonic longitudinal wave traveling through an isotropic medium is governed by the intrinsic physical properties of this medium:

$$c = \left[\frac{E(1-\varepsilon)}{\rho(1+\varepsilon)(1-2\varepsilon)} \right]^{\frac{1}{2}} \tag{1}$$

where c denotes the propagation velocity of the ultrasonic longitudinal wave, E the Young's modulus of the medium, ε the Poisson's ratio of the medium and ρ the density of the medium. When the ultrasonic longitudinal wave propagates over a distance l in the medium, the corresponding propagation time i.e., *TOF*, can be expressed as:

$$TOF = \frac{l}{c} = \left[\frac{\rho(1+\varepsilon)(1-2\varepsilon)}{E(1-\varepsilon)} \right]^{\frac{1}{2}} \tag{2}$$

from this equation, it can be deduced that for a fixed propagation distance, the superior the elastic properties of the medium (corresponding to a larger Young's modulus E) and the lower its density, the higher the propagation velocity of the ultrasonic wave and the shorter the *TOF*. During the charge-discharge process of a lithium battery, the lithium ions migrate in the electrolyte and undergo intercalation and deintercalation reactions between the cathode and anode. At the ionic level, the SOC is defined as the actual ratio of lithium ions intercalated in the electrodes (discharged state) or capable of being deintercalated from the electrodes to the total lithium ions (charged state). Therefore, changes of the SOC means the fluctuations in the electrolyte density and Young's modulus. Ultrasonic wave can precisely capture this change and reflect it through *TOF*, as Figure 1A shows.

A gel lithium battery can be regarded as a multilayer composite structure as shown in Figure 1B. Owing to the different material compositions between adjacent layers, the ultrasonic parameters within each layer also differ. To characterize this scenario, a continuous and homogeneous layered medium model is adopted to describe the propagation process of ultrasonic waves inside the battery. In each individual layer, the acoustic impedance of the material can be expressed as:

$$Z_i = \rho_i c_i = \sqrt{\frac{\rho_i E_i (1-\varepsilon_i)}{(1+\varepsilon_i)(1-2\varepsilon_i)}} \tag{3}$$

where Z denotes the acoustic impedance and i represents the layer sequence number. The battery is mainly composed of three types of layers: the separator, cathode, and anode. Since these three types of layers are arranged in a repeating sequence, the value of i ranges from 1 to 3. Acoustic impedance does not serve for independent calculation, but is used to determine the laws of ultrasonic reflection and transmission at the interface between two layers. For instance, at the interface between the separator layer and the cathode layer with acoustic impedances Z_1 and Z_2 respectively, the ultrasonic reflection coefficient r and transmission coefficient t can be expressed as:

$$r = \frac{Z_2 - Z_1}{Z_2 + Z_1} \qquad t = \frac{2Z_2}{Z_2 + Z_1} \tag{4}$$

from the above equations, it can be concluded that when Z_1 and Z_2 are identical, the reflection coefficient r equals 0, corresponding to total transmission of ultrasonic waves. In contrast, when the difference between Z_1 and Z_2 is significant, r approaches 1, indicating that most of the ultrasonic energy is reflected. For the multilayered structure, neglecting the nonlinear effects of the material, the waveform of ultrasonic waves can be assumed to remain unchanged during propagation, with only amplitude attenuation caused by multiple reflections.

 doi:10.20944/preprints202604.1476.v1

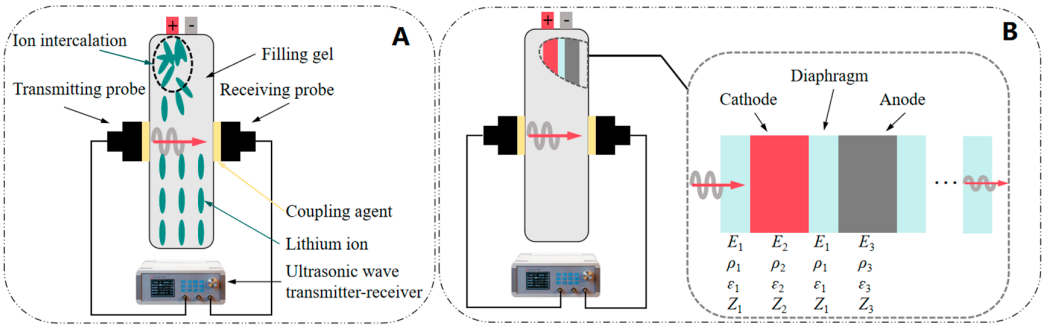

Figure 1. Ultrasonic wave passes through the gel battery: (A) Density and Young's modulus affect *TOF*; (B) Interlayer reflection affects *SA*.

In summary, the acoustic impedance of the battery is governed by the density, Young's modulus, and Poisson's ratio of each internal layer, and the intensity of ultrasonic reflection is in turn determined by the acoustic impedance. This physical relationship is directly reflected by *SA*. Meanwhile, the above three physical parameters also jointly determine the velocity of ultrasonic wave, thereby exerting a direct influence on the *TOF*. It follows that the ultrasonic propagation characteristics inside the battery are intrinsically correlated with the intrinsic physical properties of the internal materials, which demonstrates the feasibility of ultrasonic technology for SOC characterization.

2.2. Analysis of Ultrasonic Time-Domain Signals for Gel Battery SOC

In this study, two identical commercial EB-BS908 gel lithium batteries with consistent aging states are used, designated as B1 and B2, respectively. The batteries have a rated capacity of 3435 mAh, with upper and lower cut-off voltages of 4.45 V and 3.0 V. Specifically, B1 is used for ultrasonic signal analysis, while B2 acts as a validation battery for subsequent operation. The schematic diagram of the experimental setup is shown in Figure 2. A battery test system is used to monitor in real time the variations in voltage, current and temperature of the battery during charging and discharging, while an ultrasonic detection system is employed to acquire the corresponding ultrasonic signals. Throughout the experiment, the battery is placed in a constant temperature chamber with a controlled temperature 25℃. The ultrasonic longitudinal wave used in this study has a central frequency of 4.5 MHz.

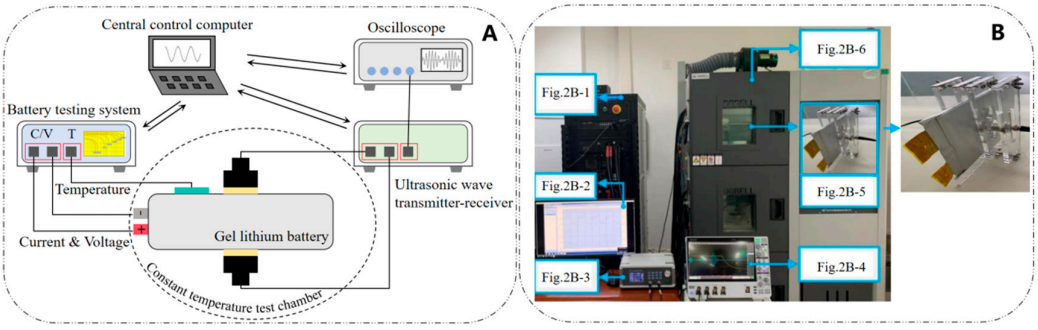

Figure 2. Battery experimental platform: (A) Schematic diagram; (B) Experimental image, 1-6 are respectively: temperature detector, upper computer, ultrasonic wave.

The ultrasonic time-domain signals during the charge-discharging cycle are shown in Figure 3 and Figure 4. Furthermore, the precise values of the *TOF* and *SA* are extracted from the time-domain ultrasonic signals, as depicted in Figure 5. As illustrated in the results, the *TOF* and *SA* of ultrasonic waves exhibit a clear correlation with the SOC during a full charge-discharge cycle. It can be observed

 doi:10.20944/preprints202604.1476.v1

that the *SA* is positively correlated with the SOC, whereas the *TOF* shows a significant negative correlation with the SOC.

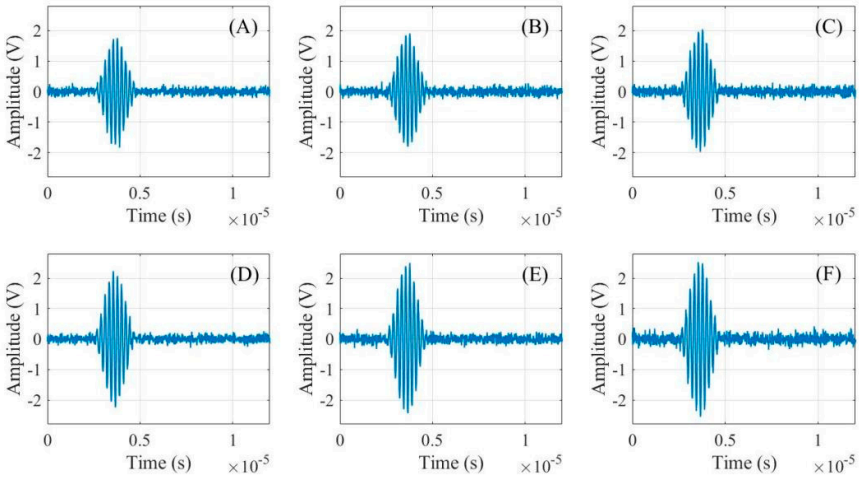

Figure 3. The ultrasonic time-domain signal during charging process: (A) SOC=0%; (B) SOC=20%; (C) SOC=40%; (D) SOC=60%; (E) SOC=80%; (F) SOC=90%.

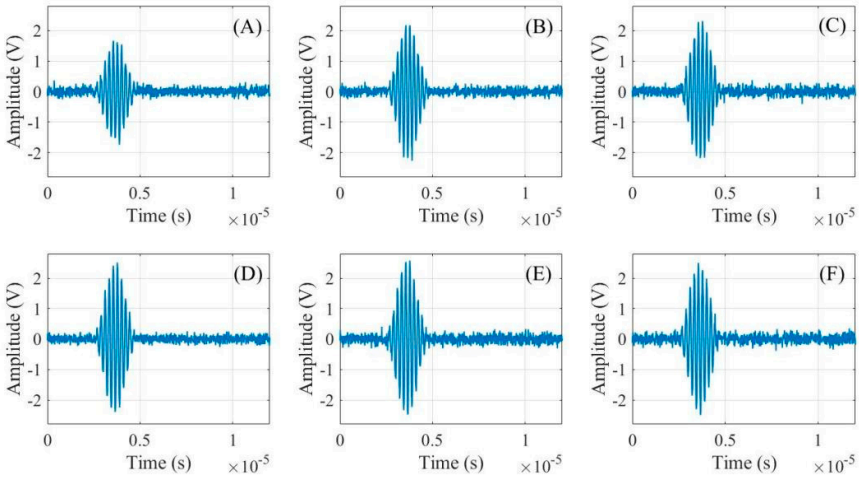

Figure 4. The ultrasonic time-domain signal during discharging process: (A) SOC=0%; (B) SOC=20%; (C) SOC=40%; (D) SOC=60%; (E) SOC=80%; (F) SOC=90%.

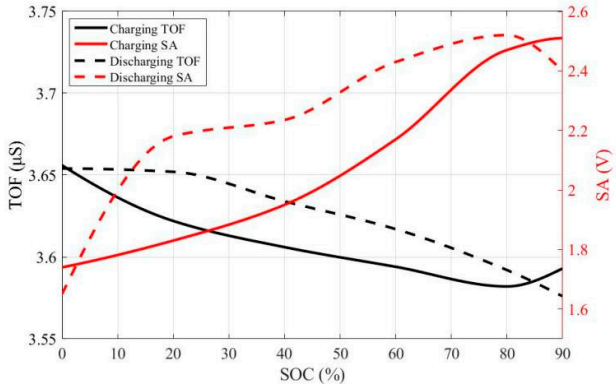

 doi:10.20944/preprints202604.1476.v1

Figure 5. The precise values of *SA* and *TOF* during the charge-discharge cycle.

At the initial charging stage, with the SOC increasing from 0% to approximately 10%, a concentration polarization phenomenon is induced inside the battery by external excitation. This leads to a significant variation in the physical properties of the internal material, accompanied by a rapid decrease in *TOF* value and a slow growth in *SA* value.

In the middle charging stage, with the SOC rising from approximately 10% to 80%, the *TOF* and *SA* exhibit entirely opposite variation trends. For the *TOF*, two competing effects act on its value during the charging process: on one hand, the increase in battery thickness elongates the ultrasonic propagation path, which tends to increase *TOF*; on the other hand, the rise in the ratio of Young's modulus to density of the battery's internal electrode material leads to an increase in ultrasonic wave velocity, which in turn exerts a *TOF*-reducing effect. The overall decreasing trend of the *TOF* indicates that the variation in the physical properties of the battery's electrode material plays a dominant role in this stage. For the *SA*, the higher the hardness and densification degree of the material, the lower its damping property and the weaker the attenuation of the ultrasonic signal. Accordingly, during the battery charging process, the increase in Young's modulus of the electrode material leads to an enhancement in material stiffness and a reduction in acoustic impedance, which consequently gives rise to an increase in *SA*. In this middle charging stage, the variations in *TOF* and *SA* exhibit a relatively uniform trend. This is attributed to the gradual achievement of a dynamic equilibrium in the migration rate of lithium ions as the constant-current charging proceeds, with the rates of electrochemical reactions and material property evolution tending to be stable.

In the late charging stage, with the SOC increasing from approximately 80% to 90%, the charging mode switches from constant current to constant voltage, and the charging current gradually declines to the preset cut-off current. Correspondingly, the migration rate of lithium ions inside the battery decreases, and the magnitude of variation in the physical properties of the electrode material is also diminished. Consequently, the *SA* continues to increase while its growth rate diminishes gradually. Owing to the reduced rate of electrochemical reactions, the variation in battery thickness exerts a dominant effect on the *TOF* relative to the changes in the physical properties of the internal materials, thereby leading to a gradual increase in *TOF*. Discharging constitutes the reverse process of charging, accordingly, the variation trends of the *TOF* and *SA* during the discharging stage are opposite to those observed in the charging stage, as illustrated in Figure 5. So the detailed analysis of this phenomenon is not presented in this study.

Overall, during the whole charging stage, the rate of change of *TOF* is approximately 40%, and that of *SA* is about 1.9%. Under the same conditions, the corresponding two values of liquid lithium battery are approximately 60% and 3.5%, respectively [17]. This difference indicates that compared to liquid battery, the two time-domain characteristics of *TOF* and *SA* are less sensitive to the SOC of the gel battery. Direct application of existing SOC estimation models based on *TOF* and *SA* has certain limitations in terms of estimation accuracy for gel battery.

2.3. Analysis of Ultrasonic Frequency-Domain Signals for Gel Battery SOC

Gel lithium batteries feature a typical layered structure. When ultrasonic waves propagate along the thickness direction of the battery, multiple reflections inevitably occur at the interlayer interfaces. Such reflections can induce the generation of harmonic waves, so the frequency characteristics of the received ultrasonic signal inherently contain the SOC information of the battery. Fast Fourier transform (FFT) is applied to the received ultrasonic signal, with the results presented in Figure 6. Here F_m denotes the amplitude corresponding to the single-frequency component with the highest intensity in the received signal, which indicates that this specific frequency component carries the maximum energy relative to other frequency components. The variation trend of F_m with the battery's SOC is generally consistent with that of *SA*. However, by eliminating the interference from other frequency components, the correlation between F_m and SOC is stronger than that between *SA*/*TOF* and SOC. Furthermore, as charging or discharging proceeds, the frequency corresponding to F_m

 doi:10.20944/preprints202604.1476.v1

varies periodically within a specific range, indicating that this frequency which corresponds to the maximum energy is not a fixed value. This phenomenon occurs because the periodic intercalation and deintercalation of lithium ions between the cathode and anode induce regular changes in the thickness and physical properties of the battery's layered structure, thereby generating distinct harmonic signals. This result verifies the feasibility of using ultrasonic signal variations to reflect the internal electrochemical processes of the battery, while also demonstrating the potential of ultrasonic waves for characterizing the SOC of gel lithium battery.

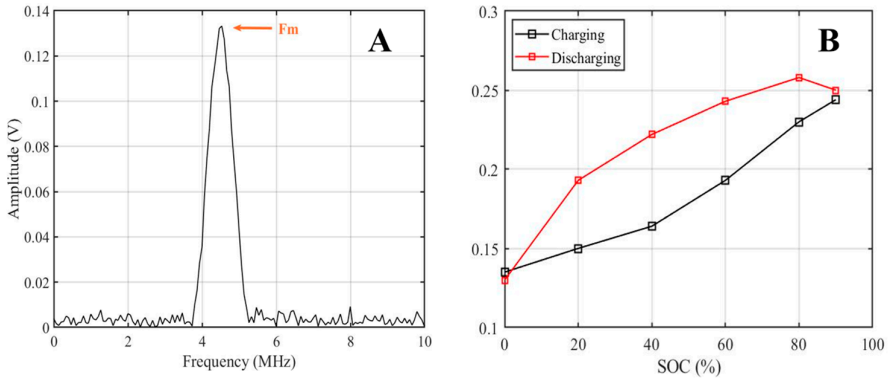

Figure 6. (A) The F_m value represents the peak of the received signal spectrum, the spectrum is from the charge process when SOC is 0; (B) The values of Fm during charge-discharge cycle.

2.4. Analysis of Ultrasonic Signal's Time-Frequency Transformation Features

The analyses presented in sections 2.2 and 2.3 demonstrate that both the time-domain and frequency-domain characteristics of the ultrasonic signal can establish a certain correlation with the SOC. Therefore, to effectively improve the accuracy of SOC estimation for gel lithium battery, it is proposed to utilize Ensemble Empirical Mode Decomposition (EEMD) to maximize the utilization of the time-frequency information contained in the ultrasonic signal. The received ultrasonic signal is processed via EEMD using the relevant toolbox in MATLAB, yielding 7 Intrinsic Mode Functions (IMFs) as shown in Figure 7.

 doi:10.20944/preprints202604.1476.v1

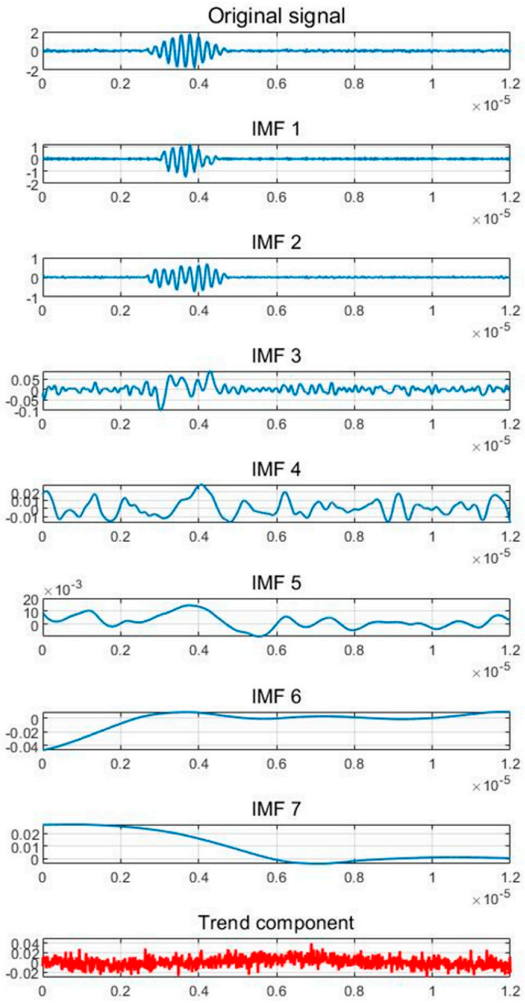

Figure 7. Schematic diagram of EEMD operation of the signal.

To further eliminate low-correlation data, the variance contribution rate (η) and correlation coefficient (γ) of the 7 IMFs are calculated. The formulas for calculating η and γ are given as follows:

$$\eta_i = \frac{\lambda_i}{\sum_{j=1}^{7} \lambda_j} \qquad \gamma_i = \frac{Cov(\lambda_i, Y)}{\sqrt{Var(\lambda_i)}\sqrt{Var(Y)}} \tag{5}$$

where λ_i represents the variance of the IMFi, Y represents the variance of the original signal, Cov(λ_i,Y) represents the covariance of λ_i and Y, Var(λ_i) and Var(Y) respectively represent the variances of λ_i and Y. The variance contribution rates and correlation coefficients of each component of the IMFs are shown in Figure 8. Obviously, the variance contribution rates and correlation coefficients of IMF1, IMF2 and IMF3 are significantly higher, thus these components contain the main information of the ultrasonic signal.

 doi:10.20944/preprints202604.1476.v1

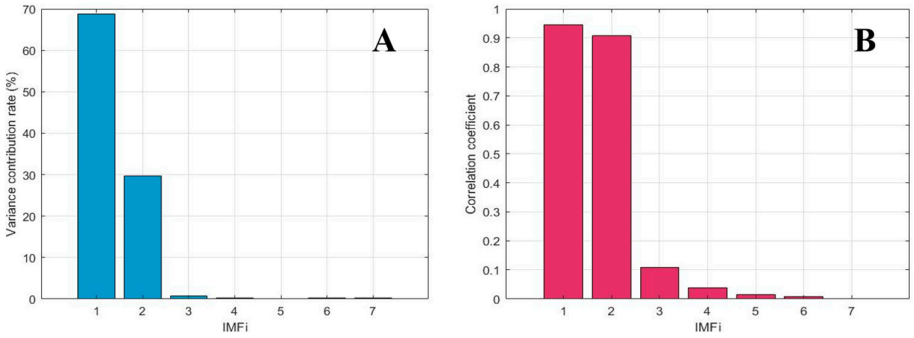

Figure 8. (A) The variance contribution rates of the 7 IMFs; (B) Correlation coefficient of the 7 IMFs.

Therefore, IMF1 to IMF3 are selected as the research objects, and their respective skewness (*s*), kurtosis (*k*), crest factor (*cf*), margin factor (*mf*), shape factor (*sf*) and impulse factor (*if*) are extracted. The results are presented in Table 1. It can be seen that the correlation coefficients between the IMFs and the six parameters differ significantly. To reduce the number of input variables, only parameters with a correlation coefficient higher than 0.8 (i.e., k_1, k_2, mf_1, mf_2, mf_3) are selected for subsequent analysis.

Table 1. Correlation coefficients between the selected parameters and SOC.

Parameter	IMF1	IMF2	IMF3
s	0.6322	0.4258	0.3361
k	0.9012	0.8344	0.4321
cf	0.7125	0.6588	0.4003
mf	0.9255	0.9012	0.8143
sf	0.6827	0.4876	0.3256
if	0.2101	0.1571	0.0145

2.5. Gel Battery SOC Eestimation Based on Ultrasonic Time-Frequency Features

The Long-Short-Term Memory (LSTM) neural networks are employed to investigate the estimation of battery SOC. The 11 characteristic values of battery B1 during charging and discharging (i.e., current, voltage, temperature, *SA*, *TOF*, F_m, k_1, k_2, mf_1, mf_2, mf_3) are normalized and used as the training set. Meanwhile, the 11 characteristic values of battery B2 with the same aging state as battery B1 are normalized and served as the test set to evaluate the performance of the SOC estimation model. During the charging and the discharging process, the sizes of the training sets are 12×202 and 12×108 respectively. To evaluate the estimation accuracy of this method, three evaluation indicators are introduced: Root Mean Square Error (RMSE), Mean Absolute Error (MAE) and Coefficient of Determination R^2. Figure 9 compares the gel lithium battery's SOC estimation obtained by the LSTM method with those by Deep Neural Networks (DNN) and Convolutional Neural Networks (CNN). Table 2 lists the three evaluation indicators under different methods. It can be observed that LSTM exhibits stronger capability in processing time-series data than DNN and CNN, thus yielding higher SOC estimation accuracy. During the charging process, the estimated SOC values are in good agreement with the reference values, with the RMSE below 0.90% and the MAE below 0.65%. At the beginning of charging, the error is relatively smaller, but as charging progresses, the error slightly increases. This reflects that LSTM can effectively capture the changes in SOC as well as the dependency path of SOC on the battery's historical state. During the discharging process, the RMSE of the estimated SOC value is within 0.42%, and the MAE is within 0.36%. As discharging processes, the error gradually decreases. Meanwhile, during the charging and discharging process, the R^2 of the established LSTM model is all above 0.99, which also indicates that when using the LSTM to estimate

 doi:10.20944/preprints202604.1476.v1

SOC, the model has a good fitting effect, strong explanatory ability for the estimated values, and high accuracy of SOC estimation.

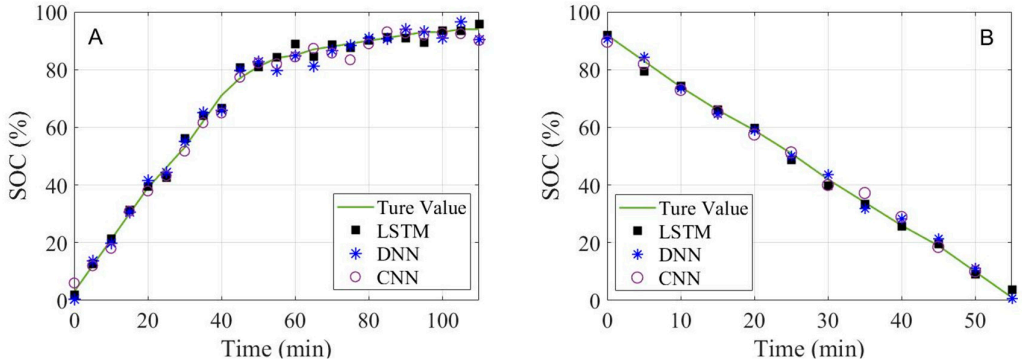

Figure 9. Comparison of LSTM, DNN and CNN in estimating the SOC of gel battery: (A) Charging process; (B) Discharging process.

Table 2. Comparison of evaluation indicators for the three methods.

Evaluation Indicator	State	LSTM	DNN	CNN
RMSE (%)	charging	0.8901	1.1043	1.3008
	discharging	0.4153	0.9933	1.2019
MAE (%)	charging	0.6419	1.0347	0.9473
	discharging	0.3541	1.1021	0.9215
R^2	charging	0.9904	0.9254	0.9016
	discharging	0.9913	0.9417	0.9570

2.5. Analysis of the Feature Choice on SOC Estimation Accuracy

To quantify the superiority of fusing multi-dimensional ultrasonic time-frequency domain features for gel battery SOC estimation, a comparative analysis is conducted on the SOC estimation accuracy of the LSTM model with different feature combinations as inputs.

(1) Traditional method: solely utilizes battery voltage, current and temperature as input features (three features in total).

(2) Integrating ultrasonic time-domain characteristics: adopts battery voltage, current, temperature and two ultrasonic signals (SA and TOF) as input features (five features in total).

The SOC estimation results for cases (1) and (2) are listed in Table3. By comparing with the data in Table 2, it can be observed that employing only voltage, current and temperature as LSTM inputs results in an SOC estimation RMSE greater than 1% and an MAE around 1%. By introducing the two extra ultrasonic time-domain features (*SA* and *TOF*) into the input set on the basis of the three conventional features, the SOC estimation RMSE remains around 1%, while the MAE is decreased to less than 1%. When all 11 features are adopted as input parameters, the SOC estimation RMSE is below 0.89% and the MAE is less than 0.65% during the charging process. The above comparative results validate the advantage the proposed method in this paper.

Table 3. Estimation accuracy under different input features.

Evaluation Indicator	State	3 features	5 features
RMSE (%)	charging	1.4020	1.2017
	discharging	1.2017	1.1340
MAE (%)	charging	1.0834	0.9301
	discharging	0.9893	0.8936
	charging	0.9214	0.9471

 doi:10.20944/preprints202604.1476.v1

R^2	discharging	0.9331	0.9601

3. Conclusions

To address the issue of insufficient accuracy in gel lithium battery SOC estimation using conventional methods that rely solely on parameters such as voltage, current, and temperature, this paper proposes a method based on the fusion of multi-dimensional ultrasonic time-frequency domain features. Firstly, a continuous uniformly layered medium model is employed to analyze the propagation characteristics of ultrasonic waves inside the battery. Then, multi-dimensional time-frequency domain features of ultrasonic signals are extracted via time-frequency analysis. Finally, combined with the LSTM neural network, a model fusing multi-dimensional ultrasonic time-frequency domain features is constructed to realize accurate SOC estimation of the gel lithium battery. The main conclusions of this paper are as follows:

(1) Multi-dimensional ultrasonic time-frequency domain features are extracted, including time-domain features, frequency-domain features and time-frequency transform features. The analysis demonstrates that these ultrasonic features can effectively characterize the electrochemical processes inside the gel battery, and eight characteristic indicators (SA, TOF, F_m, k_1, k_2, mf_1, mf_2, mf_3) exhibit a strong correlation with the battery SOC.

(2) An SOC estimation model for gel lithium battery is established based on LSTM, which fuses multi-dimensional ultrasonic time-frequency domain features. The results demonstrate that for the battery with the same aging degree, during the charging process, the SOC estimation RMSE is within 0.90% and the MAE within 0.65%; during the discharging process, the RMSE is within 0.42% and the MAE within 0.36%. The estimation results indicate that the accuracy of this method is excellent.

The findings of this study can offer an instructive reference for the condition monitoring and detection of gel batteries. Nevertheless, achieving the rapid and systematic deployment of theses research results still demands in-depth exploration and further investigation.

Author Contributions: Conceptualization, Haiyan Qiao, Guoliang Zhao; methodology, Haiyan Qiao, Guoliang Zhao; data curation and investigation, Guoliang Zhao; writing and editing, Haiyan Qiao, Guoliang Zhao and Hua Wang; project administration, Mengmeng Liu, Suzhen Liu. All authors have read and agreed to the published version of the manuscript.

Funding: This research was funded by the National Natural Science Foundation of China, grant number 52307238.

Institutional Review Board Statement: Not applicable.

Informed Consent Statement: Not applicable.

Data Availability Statement: The data generated or analyzed during this study are available from the corresponding author on reasonable request.

Conflicts of Interest: The authors declare no conflicts of interest.

References

1. Yao, J.; Kowal, J. Towards a smarter battery management system: A critical review on deep learning-based state of charge estimation of lithium-ion batteries. *Energy and AI*. **2025**, 21, 100585.
2. Hannan, M. A.; Hoque, M. M.; Mohamed, A.; Ayob, A. Review of energy storage systems for electric vehicle applications: Issues and challenges. *Renewable and Sustainable Energy Reviews*. **2017**, 69, 771-789.
3. Wei, Z.; Leng, F.; He, Z.; Zhang, W.; Li, K. Online state of charge and state of health estimation for a lithium-ion battery based on a data–model fusion method. *Energies*. **2018**, 11(7), 1810.
4. Zou, C.; Klintberg, A.; Wei, Z.; Fridholm, B.; Wik, T.; Egardt, B. Power capability prediction for lithium-ion batteries using economic nonlinear model predictive control. *J. Power Sources*. **2018**, 396, 580–589.

 doi:10.20944/preprints202604.1476.v1

5. Sultana, I.; Chen, Y.; Huang, S.; Rahman, M. M. Recycled value-added circular energy materials for new battery application: Recycling strategies, challenges, and sustainability-a comprehensive review. *Journal of Environmental Chemical Engineering*. **2022**, 10(6), 108728.
6. Peng, S.; Zhu, J.; Wu, T.; Tang, A.; Kan, J.; Pecht, M. SOH early prediction of lithium-ion batteries based on voltage interval selection and features fusion. *Energy*. **2024**, 308, 132993.
7. Sepasi, S.; Ghorbani, R.; Liaw, B. Y. A novel on-board state-of-charge estimation method for aged Li-ion batteries based on model adaptive extended Kalman filter. *Journal of Power Sources*. **2014**, 245, 337-344.
8. Suzhen, L.; Luhang, Y.; Chuang, Z. State of charge estimation of LiFeO4 batteries based on time domain features of ultrasonic waves and random forest. *Transactions of China Electrotechnical Society*. **2022**, 37(22), 5872-5885.
9. Schneider, D. Silicon anodes will give lithiumion batteries a boost. *IEEE Spectrum*. **2018**, 56(1), 48-49.
10. 2018-Omariba, Z. B.; Zhang, L.; Sun, D. Review on health management system for lithium-ion batteries of electric vehicles. *Electronics*. **2018**, 7(5), 72.
11. Zhang, M.; Fan, X. Review on the state of charge estimation methods for electric vehicle battery. *World Electric Vehicle Journal*. **2020**, 11(1), 23.
12. Hsieh, A. G.; Bhadra, S.; Hertzberg, B. J.; Gjeltema, P. J.; Goy, A.; Fleischer, J. W.; Steingart, D. A. Electrochemical-acoustic time of flight: in operando correlation of physical dynamics with battery charge and health. *Energy & environmental science*. **2015**, 8(5), 1569-1577.
13. Chang, J. J.; Zeng, X. F.; Wan, T. L. Real-time measurement of lithium-ion batteries' state-of-charge based on air-coupled ultrasound. *Aip Advances*. **2019**, 9(8).
14. Ladpli, P.; Nardari, R.; Kopsaftopoulos, F.; Chang, F. K. Multifunctional energy storage composite structures with embedded lithium-ion batteries. *Journal of Power Sources*. **2019**, 414, 517-529.
15. Chang, W.; Mohr, R.; Kim, A.; Raj, A.; Davies, G.; Denner, K.; Steingart, D. Measuring effective stiffness of Li-ion batteries via acoustic signal processing. *Journal of Materials Chemistry A*. **2020**, 8(32), 16624-16635.
16. Danko, M.; Adamec, J.; Taraba, M.; Drgona, P. Overview of batteries State of Charge estimation methods. *Transportation Research Procedia*. **2019**, 40, 186-192.
17. Liu, S.; Ren, J.; Yuan, L.; Xu, Z.; Zhang, C. Multi-Source Data Feature Extraction Method for State of Charge Estimation of LiFePO4 Battery. *Transactions of China Electrotechnical Society*. **2025**, 40(11), 3349-3361.